Nitriding of an H13 Die Steel in a Dual Plasma Reactor

O. Salas, J. Oseguera, N. Garcí, and U. Figueroa

(Submitted 11 December 2000; in revised form 21 July 2001)

The performance of a dual plasma reactor in nitriding a H13 steel was investigated and compared to other nitriding methods applied to this material. The aim was to explore the advantages of combining a weakly ionized plasma unit and a postdischarge plasma reactor to process this material. Samples of H13 were nitrided at 500, 550, and 600 °C for times ranging between 5 to 10 h. The hardness distributions obtained revealed a substantial advantage of the present method over conventional gas nitriding and some improvement over other plasma-assisted methods, especially in the development of smooth profiles. This was attributed mainly to enhanced diffusion provided by the postdischarge flow. The evolution of hardness as a function of time and temperature displayed an aging type of behavior that was related to the formation and growth of CrN as the hardening phase.

Keywords H13 steel, hardness, microstructure, plasma nitriding, surface modifications

1. Introduction

There is a continuous driving force for advances in the area of surface modification to improve tribological properties, especially for components subjected to severe wear such as dies for the Al foundry industry. In these applications, a popular candidate is the H13 steel. This steel offers high hardenability and toughness, but a relatively low wear resistance that can be improved through surface hardening treatment. The savings that result from increasing the lifetime of the dies through improvement of its wear properties have fueled several studies to optimize the surface treatments that apply to these materials. For example, Ozbaysal *et al.*[1] studied the nitriding behavior of several tool steels, including a H13 hot working steel. They found that, in all cases, the case depth increased and the surface hardness decreased with either increasing nitriding time or temperature and were practically independent of nitrogen partial pressure. A parabolic growth of the nitrided layer was observed and attributed to nitrogen volume diffusion. The evolution of hardness was related to a transformation of chromium carbides into chromium nitrides, and the resulting coherent strains between CrN and the matrix. High carbon steels showed a similar behavior to Fe-C alloys and a delayed carbide-nitride transformation. This was associated with the lower amount of nitride forming elements tied as carbides. Trejo-Luna *et al.*[2] compared the performance of conventional versus ion nitriding on several tool steels at low temperatures. According to their results, ion nitriding provides a much higher increase in hardness over conventional nitriding for the same nitriding temperature and time. They also found that ion nitriding can be carried out at a temperature as low as 150 °C. In the work of Mridha *et al.*,[3] a 3% Cr steel was gas nitrided at 470, 520, and 570 °C for times up to 36 h. They also detected the development of fine particles of CrN in the nitrided zone in the form of plates; these particles formed as a result of dissolution of prior carbides. On the other hand, Albarran *et al.*[4] studied the behavior of an H12 steel during ion nitriding at 500 °C from 2.5 to 10 h. The surface hardness in their samples increased with nitriding time up to 7.5 h and then decreased with longer treatment times. They reported a fibrous nitride phase that coarsened with treatment time, but it was not identified.

The purpose of the present study was to investigate the performance of a dual plasma reactor in nitriding H13 steel and to compare it to other methods. The dual apparatus was designed and built in our laboratory for the purpose of combining the advantages of using two sources of plasma to nitride difficult materials such as aluminum and stainless steel. The reactor incorporates a weakly ionized plasma unit that provides continuous cleaning of the sample by sputtering plus heating by ion bombarding and a post-discharge plasma reactor that supplies a highly reactive atmosphere that enhances the kinetics of the nitriding process. In the present study, we explored the extent of these advantages in the nitriding behavior of H13 steel.

2. Materials and Experimental Procedure

Samples for the nitriding experiments were cut from a rectangular H13 annealed steel bar. The composition of the bar was within the nominal values: 0.32 to 0.45% C, 0.20 to 0.50% Mn, 0.80 to 1.20% Si, 4.75 to 5.50% Cr, 1.10 to 1.75% Mo, and 0.8 to 1.20% V. The dimensions of the H13 plates were 4 cm long, 3 cm wide, and 1.5 cm thick. Prior to nitriding, the samples were quenched and tempered in the following conditions: austenizing at 1020 °C for 2 h, cooling in forced air to room temperature and then two tempering treatments at 540 °C for 2 h each, followed by forced convection cooling. The resulting microstructure had a hardness of 52 Rc, and it basically consisted of tempered martensite plus carbides. The decarburized layer that formed at the surface during heat treatment was removed by grinding. The surface of the sample to be exposed to the nitriding atmosphere was polished to mirror finish with diamond paste.

The nitriding treatments were performed in the reactor

O. Salas, J. Oseguera, N. García, and **U. Figueroa,** Instituto Tecnológico y de Estudios Superiores de Monterrey-CEM-DIA, Departamento de Ingeniería Mecánica, Carretera a Lago de Guadalupe km. 3.5, Atizapán, México, 52926 México. Contact e-mail: osalas@campus.cem.itesm.mx.

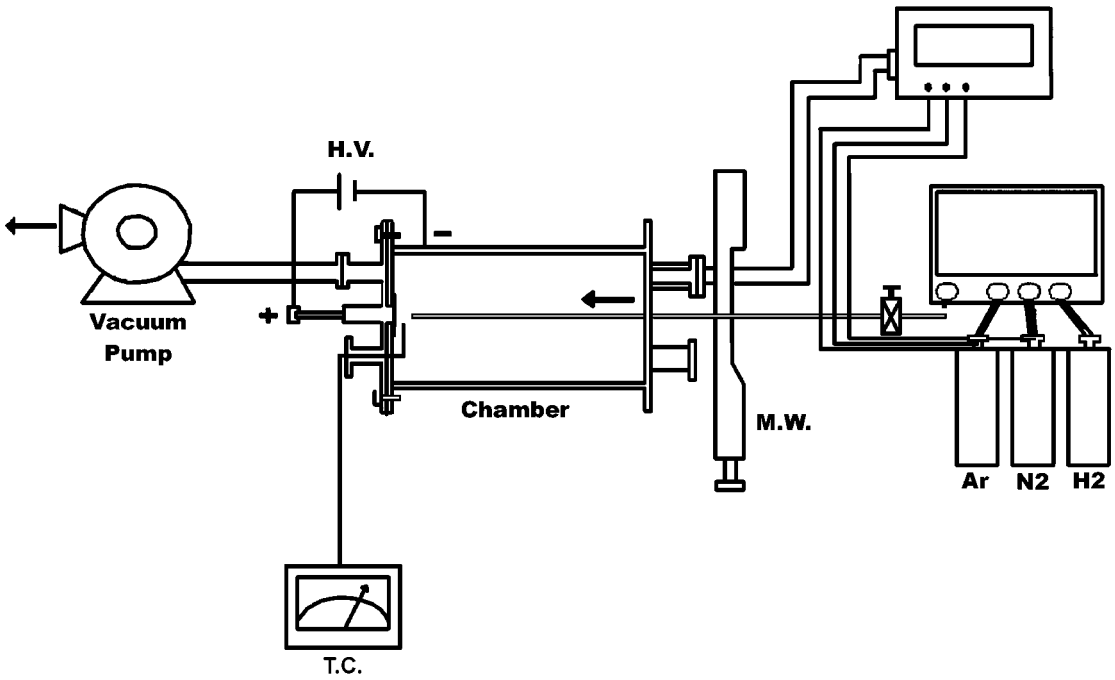

Fig. 1 Schematic drawing of the dual plasma reactor showing its main components

shown schematically in Fig. 1. As mentioned, the salient features of this apparatus are the two sources of plasma used to carry out the surface treatments: a weakly ionized plasma and a postdischarge plasma source. The nitriding experiments consisted of two basic steps: a cleaning-heating stage done by the weakly ionized plasma and the actual nitriding stage with the postdischarge flow of the microwave generated plasma. The nitriding treatment was started by introducing the sample in the dual reactor followed by evacuation of the chamber. After a pressure of 240 Pa was reached (in about 50 min), a gas mixture of 30 sccm Ar + 80 sccm H_2 was introduced into the chamber and a voltage of 320 V was applied to generate the weakly ionized plasma. Shortly after the discharge was stabilized, the microwave plasma was induced with working and reflected powers of 140 and 43 W, respectively. Upon reaching 450 °C in these conditions, a flow of 190 sccm of N_2 was introduced to start the nitriding treatment. The working pressure at this point increased to 780 Pa, and the voltage was adjusted to maintain the desired temperature. During this period, the reflected power decreased to 25 W, and, at this point, the nitriding time began to be recorded. After the treatment time was completed, the reactor was shut down, and the sample was taken out to cool by forced convection.

Specimens were obtained for cross-sectional analysis by optical and scanning electron microscopy plus energy dispersive spectroscopy. The surface of the samples was analyzed by x-ray diffraction, both with and without the surface white layer, in order to analyze the phases that formed below in the diffusion zone. The white layer was carefully removed by controlled polishing with 6 μm diamond paste. For microscopic observation, the nitrided samples were etched with Nital 2. Vickers microhardness profiles were obtained from the cross sections with a load of 50 g. For each depth, at least five hardness values were obtained. Rockwell surface hardness was measured with a load of 15 N. Five surface values were also obtained for each sample.

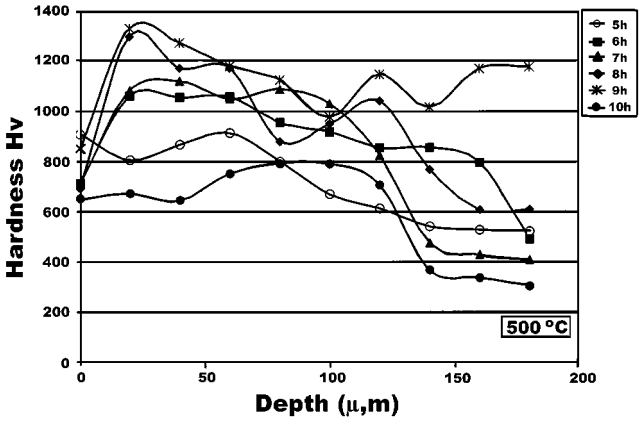

Fig. 2 Hardness profiles as a function of time for samples nitrided at 500 °C

3. Results and Discussion

3.1 Microhardness Profiles

Figures 2 to 4 show the evolution of the microhardness for the three nitriding temperatures. Even at 500 °C and short nitriding times, there was a substantial increase in hardness over the matrix values, as can be seen by comparing the profiles to Fig. 5, which shows the change in matrix hardness as a

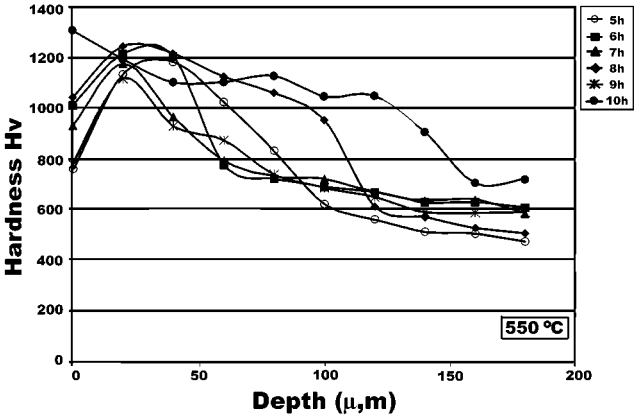

Fig. 3 Hardness profiles as a function of time for samples nitrided at 550 °C

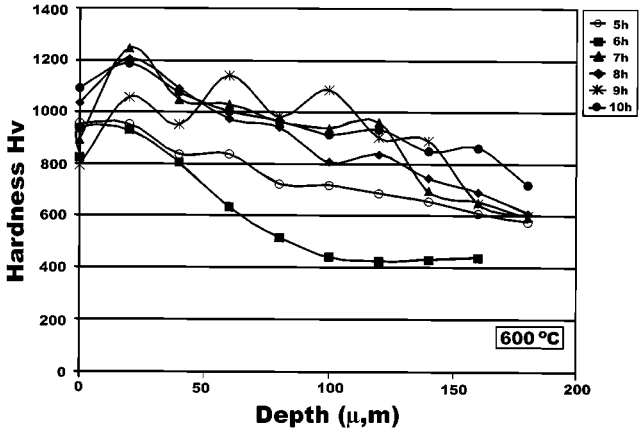

Fig. 4 Hardness profiles as a function of time for samples nitrided at 600 °C

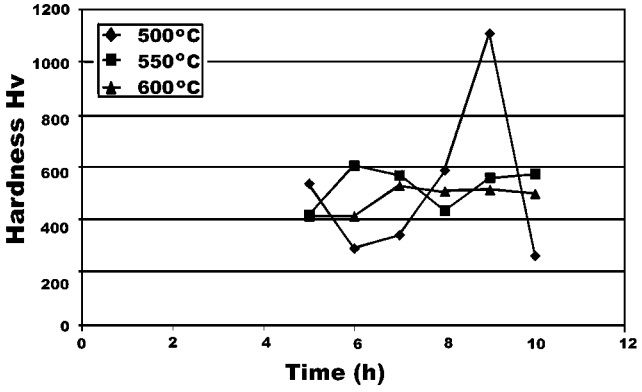

Fig. 5 Evolution of the matrix hardness with time for the three nitriding temperatures

function of time. The maximum values in hardness were not located at the surface, but at some depth below, very close to 20 μm, for all temperatures and times. After this subsurface peak, most of the curves showed a monotonic decrease of hardness with depth, although some of them displayed additional maximum at deeper locations; an extreme case was the sample nitrided for 9 h at 600 °C, which showed a serrated profile. These figures also display the effect of temperature and time on the hardness distribution after nitriding. The highest hardness values were not found at 600 °C, but at 500 °C. Also, the lower the treatment temperature, the longer the time to produce the maximum hardness, as can be readily seen in Fig. 6: 7 h for 600 °C, 8 h for 550 °C, and 9 h for 500 °C. On the other hand, the higher the nitriding temperature, the flatter and deeper the hardened layer (case depth). The effect of time can also be observed in Fig. 2 to 4, which show that the evolution of the hardness profiles was not the same for the three temperatures. For 500 °C, the level of the profiles increased with nitriding time and then abruptly decreased at 10 h. For 550 °C, the highest profiles were observed at 5 and 6 h, and, thereafter, remained relatively constant only to decrease at 9 h. For 600 °C, the profiles start at a lower level than those for the other two temperatures and then increase somewhat, but always below one of the other two. Nitriding at 500 °C produced the largest variation in hardness as a function of time, while the samples nitrided at 550 and 600 °C reached a relatively constant level after ~7 h of treatment. Furthermore, the longest treatments did not result in the highest hardness values, although they produced the deepest profiles. All these observations suggest that the hardening process during nitriding of H13 steel follows a behavior akin to aging. This opens the possibility of controlling the properties of nitrided H13 pieces with the help of aging curves developed for this process.

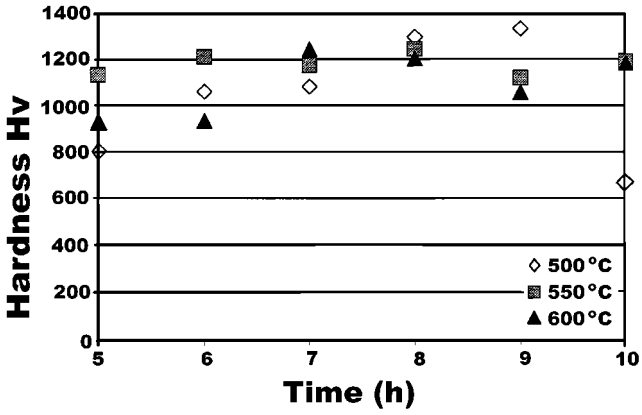

Fig. 6 Evolution of the hardness values at 20 μm depth for the three nitriding temperatures

The above observations also suggest that 500 °C may be the most suitable nitriding temperature for H13; not only because it yields the maximum hardness values and the most extensive case depths with a good hardness level, but also because it produces the largest variation in hardness as a function of time, which, in turn, offers a wide range of time to control the case depth hardness. Also, the higher hardness values at 500 °C for 8 and 9 h may indicate that the samples nitrided at 600 °C should be treated for shorter times to reach a similar hardness level.

Comparing the present hardness results with those obtained by other techniques, it can be said that, in general, the present nitriding method produces comparable or better results in shorter times. The most remarkable difference is found when

the performance of the dual reactor is compared with conventional gas nitriding. Gas nitriding is usually carried out around 527 °C for 10 to 90 h in order to produce adequate case depths according to Ref 5, while, in the present method, the time to produce similar layers is considerably reduced and can be as short as 5 h. The advantage of the present method over gas nitriding is confirmed after comparing our results with those of Mridha *et al.*[3] They nitrided a Cr-Mo-V steel in a gaseous atmosphere at 520 °C for 12 h and obtained a maximum hardness of 1000 HV and a rather sharp hardness profile. This is in contrast with the higher values in hardness and the flatter profiles obtained in the present study. This is probably one of the main advantages of using the dual plasma reactor. The highly enriched nitriding atmosphere provided by the postdischarge unit results in a rapid development of high nitrogen concentrations at the sample surface.[6] This, in turn, results in higher diffusion rates, which permit penetration of nitrogen to larger depths at comparable process conditions. When compared to other plasma-assisted methods, the present technique shows improvement in several cases and at least comparable results in others. For example, in the work of Lee *et al.*,[7] both plasma nitriding and calorizing plus plasma nitriding treatments were performed on H13 samples. Their results from only plasma nitriding are similar to our results in terms of the level of hardness and shape of the case hardened layer. Also, in the work of Albarrán *et al.*,[4] where ion nitriding of an H12 steel at 500 °C was carried out for times between 0.5 and 10 h, comparable hardness results were obtained. For example, maximum hardness values on the order of 1200 HV were reached in their work, which are almost as high as the maximum values obtained in the present work. Furthermore, it should also be considered that their H12 steel contains tungsten, which is absent in H13. The presence of this element may provide additional hardening through secondary precipitation of tungsten carbides at the temperatures considered. A clear improvement in the present method was found after comparing this study with the results of the Ozbaysal *et al.*[1] In their work, several tool steels, including an H13, were ion nitrided at temperatures between 400 and 520 °C for times ranging between 2 and 12 h. In the case of the H13 steel, the maximum hardness reported was 1075 HV after nitriding for 7 h at 480 °C and the hardened case was rather shallow, on the order of 60 μm with an abrupt decrease in hardness at around this depth. In summary, the present method definitely can be used advantageously over conventional gas nitriding and may offer some improvement over other plasma-assisted methods, especially in the attainment of flatter hardness profiles that are less likely to develop residual stresses in the hardened layer. The main contribution of the dual reactor is probably the enhanced diffusion provided by the highly reactive postdischarge flow.

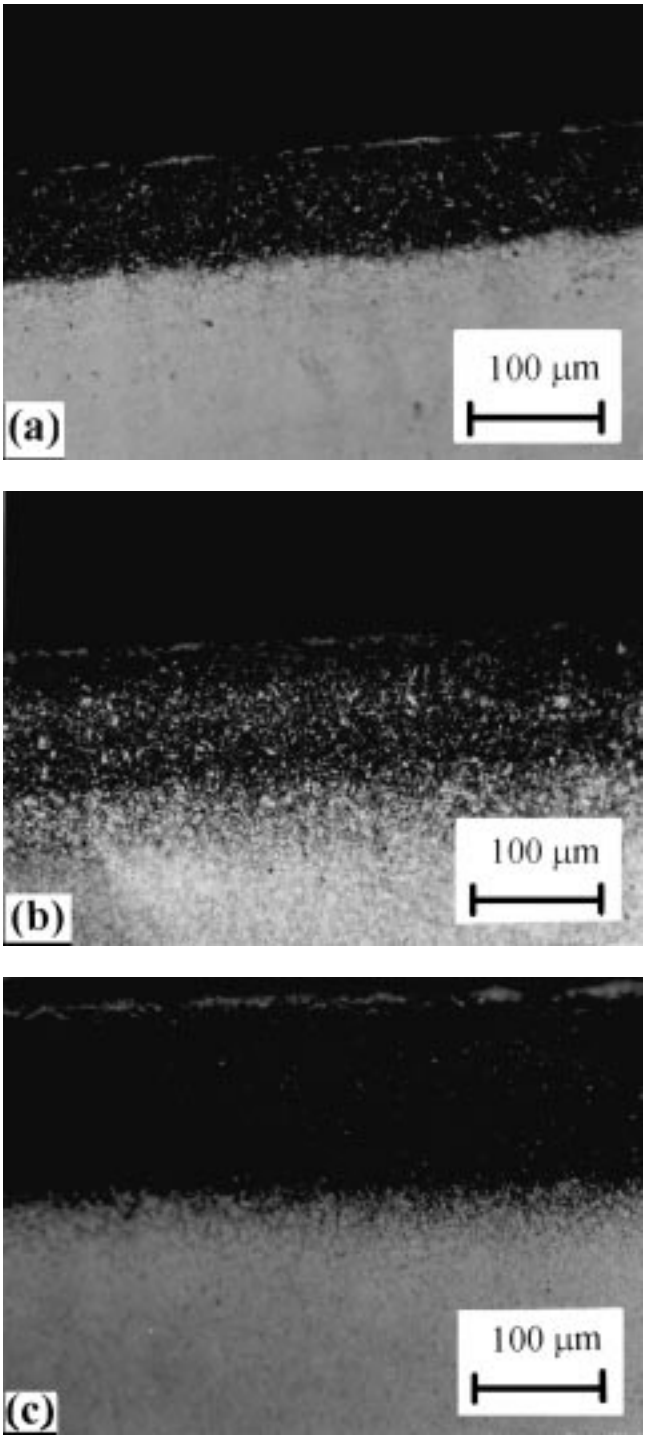

Fig. 7 Evolution of the case depth with time for samples nitrided at 550 °C: (**a**) 6 h, (**b**) 8 h, and (**c**) 10 h

3.2 Case Depth

Figure 7 is a series of optical micrographs that show the evolution of the case depth as a function of time for 550 °C. The expected increase in case thickness with time displayed in these pictures was observed for the three temperatures. Although the pictures show a rather sharp change in brightness between the hardened layer and the core structure, the hardness profiles indicate that the transition between the two structures is rather gradual, so it is difficult to measure the case depth on the micrographs. Thus, in order to further analyze the evolution of the case depth, the following criterion was used: the case depth was measured as the depth where the hardness was 50 HV above the matrix hardness for each sample. The values obtained in this fashion are presented in Fig. 8, which includes graphs of the case depth squared as a function of nitriding

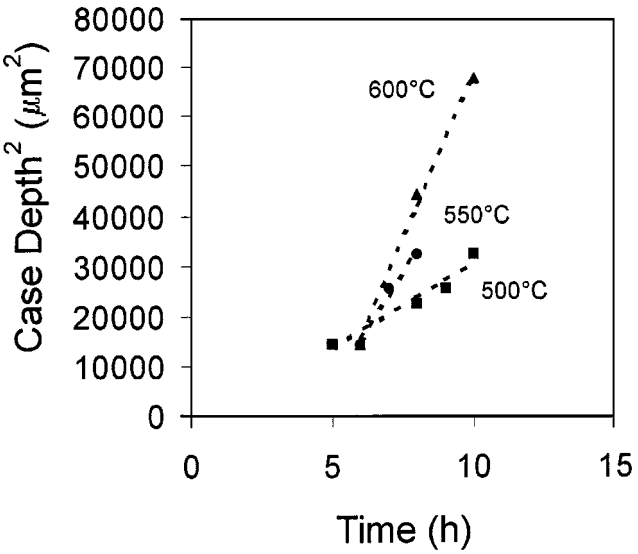

Fig. 8 Case depth as a function of time for the three nitriding temperatures

time for the three temperatures considered. The data for each temperature fit well a straight line, which indicates the parabolic nature of the layer growth and suggests a diffusion-controlled process.

3.3 Microstructural Characterization

The typical microstructure of the nitrided layer is shown in Fig. 9. The top surface, displayed in Fig. 9(a), basically consists of the white layer atop followed by a mixture of tempered martensite plus elongated precipitates formed parallel to the surface. The phases in the white layer display an acicular morphology, as shown in Fig. 9(b), and were identified as $\gamma' + \varepsilon$ by x-ray diffraction (Fig. 10a). The mixture of tempered martensite plus elongated precipitates remains essentially the same in the rest of the diffusion zone, as shown in Fig. 9(c), which corresponds to the microstructure at a deeper distance from the surface. The long precipitates have been reported by Mridha *et al.*[3] to form along former austenite grain boundaries during nitriding and to be composed of Fe_3C. However, no peaks from this phase were observed in the diffractograms taken from samples where the white layer had been removed. Remarkable deviations from the layer structure described above did develop in some samples and are currently analyzed in further detail. A sample that particularly stands out is the one nitrided at 500 °C for 9 h, which also displayed an outstanding hardening behavior. Preliminary results show a completely different morphology of the phases formed during nitriding of this sample. To identify the hardening phases in the nitrided samples, x-ray diffraction patterns were obtained from the zone below the white layer. Figure 10 displays the x-ray diffraction results from the sample nitrided at 550 °C for 8 h. The upper figure corresponds to the surface of the nitrided sample with the white layer, while the bottom pattern represents the surface obtained after the layer was removed. Before the white layer is removed, only $\varepsilon + \gamma'$ appears in the diffractogram due to the large thickness of this layer, which greatly absorbs the x-rays. However, below the white layer, Fig. 10(b) shows the

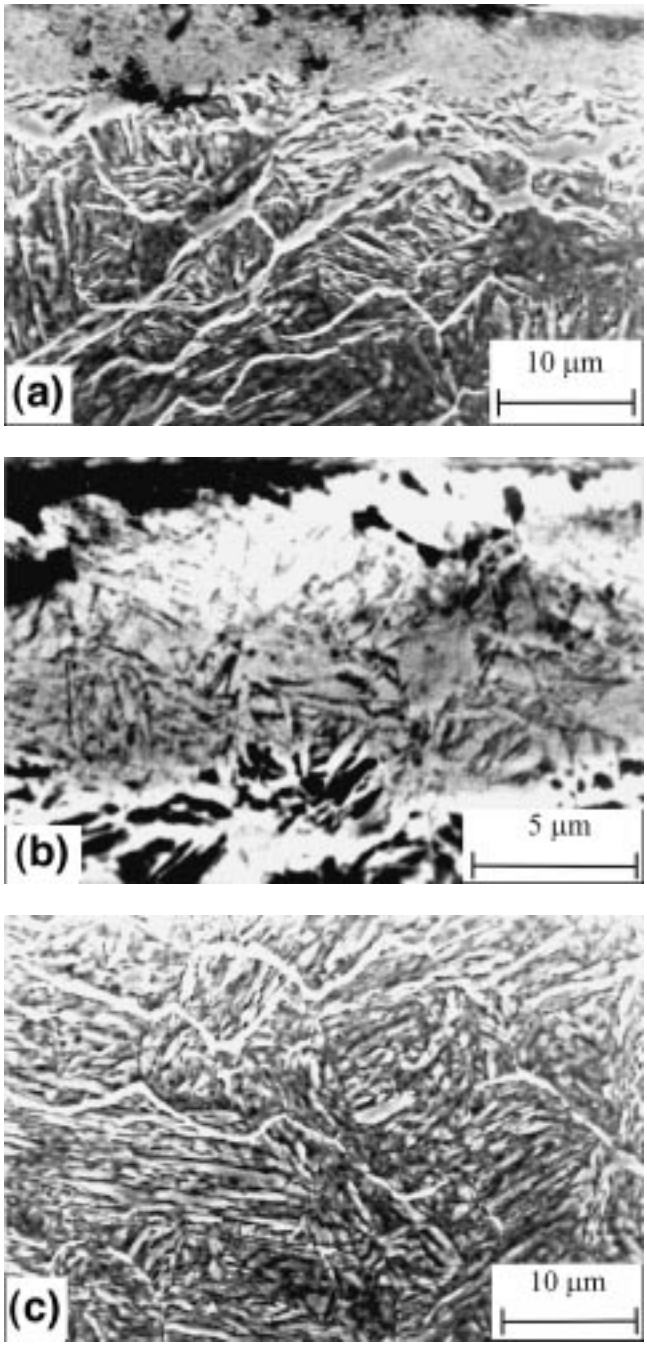

Fig. 9 Scanning electron microscopy pictures showing the microstructure of the hardened case: (**a**) surface structure, (**b**) structure of the white layer, and (**c**) structure in the diffusion zone

presence of mostly CrN plus some weak peaks of ferrite. Further analysis by transmission electron microscopy confirms the presence of a fine distribution of CrN precipitates near the surface, as shown in Fig. 11. This figure includes a bright-field image and the corresponding diffraction pattern from the surface of the sample nitrided for 8 h at 600 °C. The bright-field image displays the presence of a fine distribution of dark precipitates whose small size is confirmed by the ring diffraction pattern obtained from this area. The aging behavior displayed in the hardness

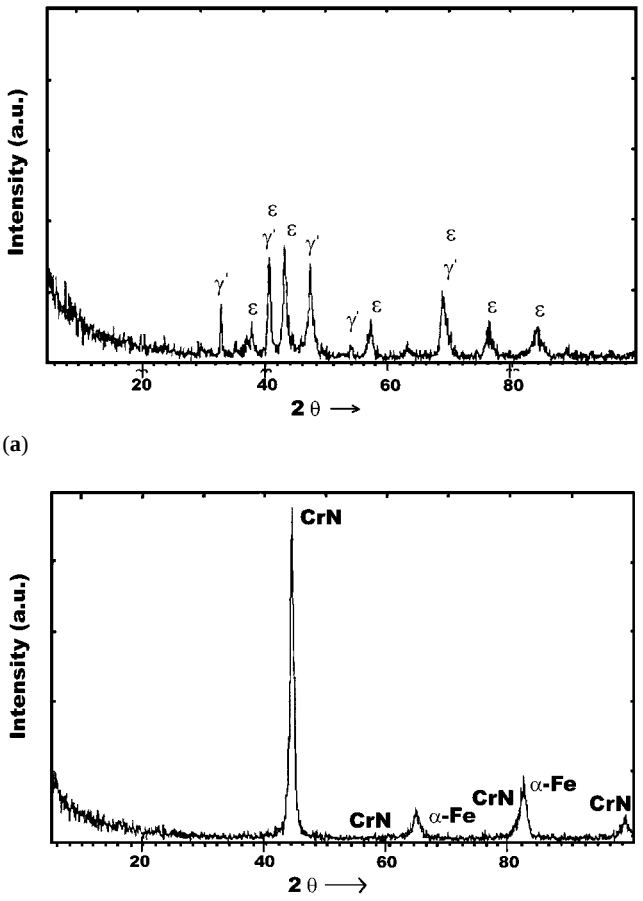

Fig. 10 X-ray diffraction patterns obtained from the sample nitrided at 550 °C for 8 h: (**a**) pattern from the original surface and (**b**) pattern after the white layer was removed

curves can now be related to the formation of CrN during nitriding. At short times, there is not enough of this phase to result in a high value of hardness; however, at intermediate times, there is an optimum amount, size, and distribution of CrN, which, after longer treatment times, coarsens and results in a new drop in the hardness values.

4. Conclusions

Nitriding of an H13 die steel in the dual plasma reactor offers a substantial advantage over conventional gas nitriding. It results in higher hardness levels and much shorter nitriding times. In respect to other plasma methods, the dual reactor may produce similar or higher hardness distributions and, more importantly, flatter hardness profiles. The improvement observed with the dual reactor is mainly attributed to the highly reactive post-discharge flow involved. This flow rapidly produces high nitrogen concentrations at the surface, which, in turn, result in enhanced diffusion and layer growth rates. The hardening process exhibited an aging type of behavior that was associated with the formation, growth, and coarsening of CrN nitrides.

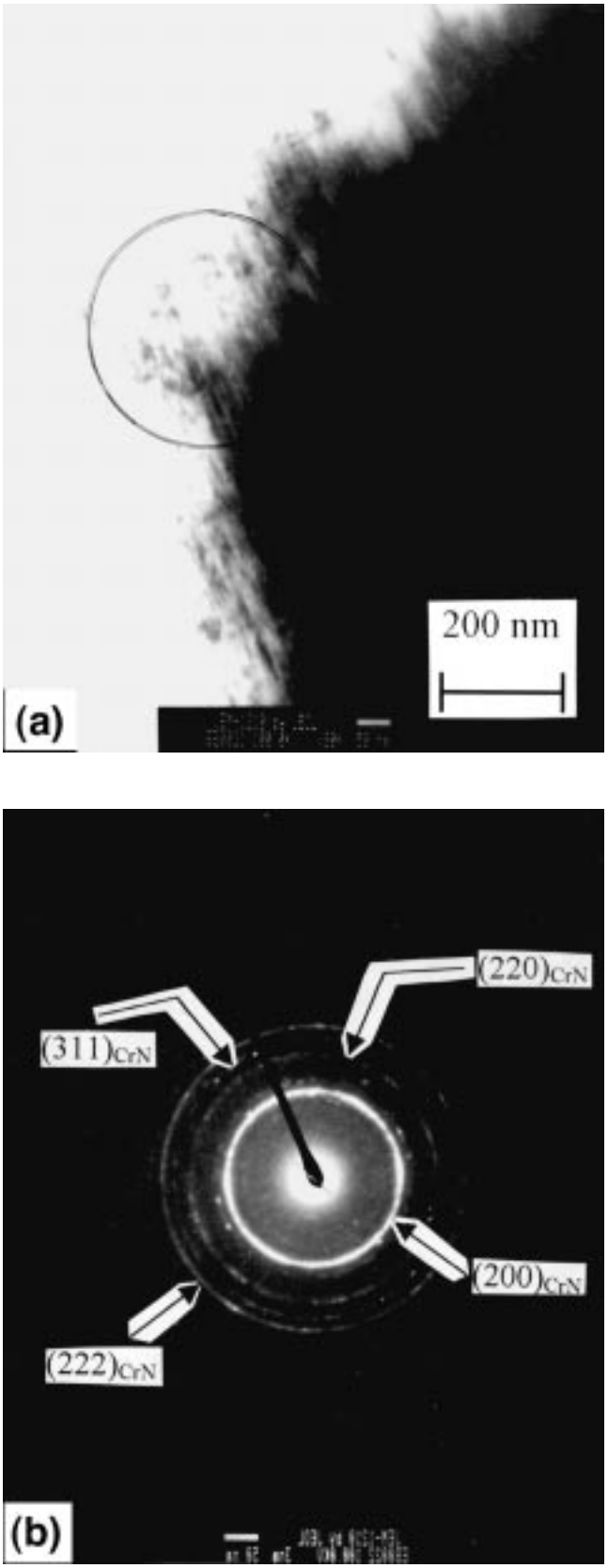

Fig. 11 Transmission electron microscopy images of the sample nitrided for 8 h at 600 °C: (**a**) bright-field image and (**b**) selected area diffraction pattern of the circled area in (a)

Acknowledgments

We greatly appreciate the help of Ms. Thelma Falcón, ININ-México, and Ms. Georgina Flores, UAM-Atzcapotzalco-México, with the x-ray diffraction work.

References

1. K. Ozbaysal, O.T. Inal, and A.D. Romig: *Mater. Sci. Eng.*, 1986, vol. 78, pp. 179-91.
2. R. Trejo-Luna, E.P. Zironi, J. Rickards, and G. Romero: *Scripta Metall.*, 1989, vol. 23, pp. 1493-96.
3. S. Mridha and D.H. Jack: *Met. Sci.*, 1982, vol. 16, pp. 398-404.
4. J.L. Albarran, J.A. Juárez-Islas, and L. Martínez: *Mater. Lett.*, 1992, vol. 15, pp. 68-72.
5. *Metals Handbook, Desk Edition*, 2nd ed., J.R. Davis, ed., ASM International, Materials Park, OH, 1998, pp. 355-57.
6. J. Oseguera, O. Salas, U. Figueroa, and M. Palacios: *Surf. Coating Technol.*, 1997, vol. 94–95, pp. 587-91.
7. S.Y. Lee, J.W. Chung, C.W. Kim, J.G. Han, S.S. Kim, and J.H. Lee: *Surf. Coating Technol.*, 1997, vols. 94–95, pp. 272-78.